Chapter VI

QSAR studies of Anthrax Lethal inhibitors through Quantum Chemical Indices

6.1: Introduction

Bacillus Anthracis is a gram positive, rod shaped spore- forming bacterium that causes infectious disease Anthrax [**1**]. The bacterium secreted three proteins protective antigen (PA), which is a pore forming sub unit; edema factor (EF), which is an adnylatecyclase that increases c AMP levels in cells and lethal factor (LF), which is a protease that cleaves mitogen activated protein kinase - kinase family [2-5]. These three proteins are individually non toxic but assemble to form two toxic complex, lethal toxin, and edema toxin [**6**]. Initially PA binds to host cell surface and cleaved by a cell associated furine type protease to form PA63 [7-10]. Then PA63 oligomerizes in to a heptameric pore-forming complex to which LF and EF bind [11]. The resulting pore-forming complex is internalized by receptor-mediated endocytosis and is trafficked in to a low pH endosome . Then complex undergoes a conformational change that allows the EF and LF to translocated in to the host cell cystol and exert their toxic action [12-14]. Inside the cystol, LF is then able to cleave mitogen activated protein kinases kinases (MAPKK) and disrupting interaction with mitogen activated protein kinase, which in turn results in inhibition of the signaling path way [15-17]. Hydroxamate analogues are used as inhibitors of the anthrax lethal toxin [18].

In this paper, we developed six QSAR models by stepwise regression analysis with respect to their experimental value of lnIc50. The method is very useful in elucidating the mechanism of chemical and biological interaction in various biomolecules. The QSAR approach employs thermodynamically derived and computational based descriptors to correlate biological activity (lnIc50) in isolated receptors. Three standard quantum chemical descriptors routinely used in QSAR analysis are quantum, electronic, surface and steric. For screening of chemical database or virtual libraries before their synthesis,

the use of QSAR models appears equally attractive to chemical manufacturers, pharmaceutical companies.

6.2: Materials and Methods

Structural and biological data of hydroxamate analogue was collected from site Binding db (www.bindingdb.org) as shown in Table 1 [19-21]. Structure of Hydroxamate analogue is represented in Figure 1.

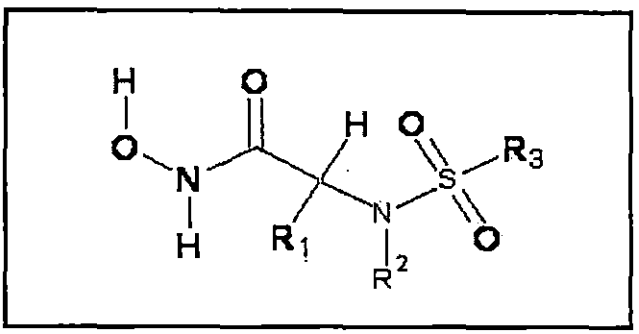

Figure 1: Structural representation of Hydroxamate analogue

Table 1: Chemical structure of Hydroxamate analogue by substituting R1, R2, R3 of figure 1.

Compd No.	R1	R2	R3
1	$-CH(CH_3)_2$	-H	$4-C_6H_4-OCH_3$
2	$-CH(CH_3)_2$	$4-CH_2$-Pyrdinyl	$4-C_6H_4-OCH_3$
3	$-CH(CH_3)_2$	3-CH_2CH_2Thiophenyl	$4-C_6H_4-OCH_3$
4	$-CH(CH_3)_2$	1-CH_2-CH_2-Imidazoly	$4-C_6H_4-OCH_3$
5	$-CH(CH_3)_2$	-H	C_6H_5
6	$-CH(CH_3)_2$	-H	$2-F-C_6H_5$
7	$-CH(CH_3)_2$	-H	$3-Cl-C_6H_5$
8	$-CH(CH_3)_2$	-H	$4-F-C_6H_5$
9	$-CH(CH_3)_2$	-H	$4-CH_3-C_6H_5$
10	$-CH(CH_3)_2$	-H	$3-CH_3-C_6H_5$

Compd No.	R1	R2	R3
11	$-CH(CH_3)_2$	-H	4-F-3-CH_3-C_6H_5
12	$-CH(CH_3)_2$	-H	3-F-4-CH_3-C_6H_5
13	$-CH(CH_3)_2$	-H	$-CH_2-CH_2-C_6H_5$
14	$-CH(CH_3)_2$	-H	3-Chloro- benzyl
15	$-CH(CH_3)_2$	-H	4-Hydroxy-3-methyl- C_6H_5
16	$-CH(CH_3)_2$	-H	4-Fluoro-3-hydroxymethyl-C_6H_5
17	$-CH(CH_3)_2$	-H	4-Fluoro-2-hydroxymethyl-C_6H_5
18	$-CH(CH_3)_2$	-H	2-Chloro-5-Thiophenyl
19	$-CH(CH_3)_2$	-H	2-{5-(1,2,3-Thiadiazolyl)-thiophenyl
20	$-CH_3$	-H	4-Fluro -3-methyl - C_6H_5
21	$-CH_2CH_3$	-H	4-Fluro -3-methyl - C_6H_5
22	$-(CH_2)_3CH_3$	-H	4-Fluro -3-methyl - C_6H_5
23	$-C(CH_3)_3$	-H	4-Fluro -3-methyl - C_6H_5
24	Cyclopropyl	-H	4-Fluro -3-methyl - C_6H_5
25	Cyclobutyl	-H	4-Fluro -3-methyl - C_6H_5
26	Cyclopentyl	-H	4-Fluro -3-methyl - C_6H_5
27	Cyclohexyl	-H	4-Fluro -3-methyl - C_6H_5
28	Phenyl	-H	4-Fluro -3-methyl - C_6H_5
29	Cyclohexyl	-H	4-Fluro -3-methyl - C_6H_5
30	3-Tetrahydrofuranyl	-H	4-Fluro -3-methyl - C_6H_5
31	$-CH_2(CH_3)CH_2CH_3$	-H	4-Fluro -3-methyl - C_6H_5
32	$-CH_2(CH_3)CH_2CH_3$	-H	4-Fluro -3-methyl - C_6H_5
33	2-(Cyclopropyl)Methyl	-H	4-Fluro -3-methyl - C_6H_5
34	2-(1Cyclopropyl)Ethyl	-H	4-Fluro -3-methyl - C_6H_5

The QSAR studies were carried out using 34 compounds of hydroxamate analogue. The statistically significant model was constructed from training set by using eight

parameters. The data set was divided in to training set of 25 compounds and test set of 9 compounds on the basis of their activity.

Quantum chemical descriptors namely HOMO, LUMO, dipole moment (DM) were calculated using GAMESS [22]. van der Waals surface area (VSA) , molar refractivity (MR), solvent accessible surface area (SASA), polarizability (POL), Partition coefficient (logP) were calculated using Mervin logP calculator. The 2D geometry of compounds was drawn in ChemSketch and converted into 3D model in 3D viewer. Energy minimization was done under MOPAC module according to AM1 (Austin Model 1) method using RHF (restricted HartreeeFock: closed shell) wave function.

6.3: Results and Discussion

The values of quantum chemical indices and natural logarithm of experimental IC_{50} value of training set is given in Table 2 and test set is given in Table 6. Correlation matrix for descriptors of training set given in Table 3

Table 2: Values of quantum chemical indices and experimental value of $lnIC_{50}$ of training set

Compd	VSA	MR	SASA	POL	logP	HOMO	LUMO	DM	$lnIC_{50}$
1	6.0866	4.2868	6.24	3.3996	0.961	-0.2462	-0.0339	6.7728	6.8024
2	6.3491	4.6061	6.3343	3.6623	1.315	-0.2135	-0.0433	6.4262	8.0392
3	6.1647	4.6454	6.1191	3.7402	2.598	-0.1933	-0.0414	4.2424	7.6497
4	6.3631	4.6009	6.4264	3.6855	0.888	-0.2045	-0.0367	9.1421	9.8574
5	5.9753	4.1938	6.1289	3.2883	0.904	-0.2298	-0.0448	7.7259	7.0031
6	5.796	4.1975	6.1255	3.2846	1.02	-0.2438	-0.0542	7.6089	8.7948
7	5.7643	4.1975	5.8296	3.2915	1.044	-0.1461	-0.039	8.3645	7.9374
8	5.8181	4.1975	5.9459	3.2918	1.068	-0.2156	-0.0582	8.4473	5.6699
9	6.0542	4.2671	6.2168	3.3706	1.353	-0.2406	-0.0408	5.1837	8.0064
10	6.053	4.2671	6.2184	3.3639	1.329	-0.2204	-0.0462	7.4782	5.9915
11	6.0678	4.2701	6.2316	3.363	1.444	-0.2451	-0.0482	7.3547	4.8675

12	5.8508	4.2701	5.9275	3.3734	1.444	-0.2175	-0.0488	5.5005	8.5526
13	5.902	4.3257	5.9437	3.433	1.175	-0.2247	-0.0119	6.2454	9.3826
14	5.8832	4.3263	5.9283	3.4306	1.62	-0.1225	-0.0371	1.6783	9.7172
15	6.0742	4.2945	6.2261	3.3911	1.269	-0.2056	-0.0212	7.5077	7.4025
16	5.8734	4.2946	5.9116	3.3995	0.334	-0.1566	-0.0475	1.932	6.3969
17	6.0869	4.2946	6.1758	3.3814	0.334	-0.2394	-0.0508	5.6045	7.1778
18	5.7072	4.1821	5.7949	3.3595	1.654	-0.2527	-0.0526	1.8346	7.1778
19	6.0945	4.4011	6.2802	3.4391	1.487	-0.2492	-0.0761	4.8421	6.697
20	5.9221	4.1357	6.1201	3.2122	0.665	-0.2543	-0.0376	1.5427	4.8675
21	5.7737	4.2056	5.8657	3.2995	1.201	-0.245	-0.0398	1.4663	4.6052
22	6.1395	4.3342	6.3489	3.4447	2.265	-0.2482	-0.0377	3.2164	4.2485
23	5.9504	4.3298	6.0264	3.3986	2.025	-0.2035	-0.0571	8.362	5.7038
24	6.0125	4.2446	6.1579	3.3285	1.192	-0.2037	-0.0532	7.8314	4.7875
25	6.0789	4.3085	6.2031	3.4004	1.366	-0.1316	-0.0342	3.3367	4.8675

Table 3: Correlation matrix for descriptors of training set

	VSA	**MR**	**SASA**	**POL**	**logP**	**HOMO**	**LUMO**	**DM**	**lnIC$_{50}$**
VSA	1	0.7762	0.895	0.7289	0.1426	-0.0477	0.1194	0.264	0.0643
MR	0.7762	1	0.4965	0.9837	0.377	0.1856	0.0786	0.1178	0.3652
SASA	0.895	0.4965	1	0.432	0.0624	-0.2605	0.0133	0.3181	-0.0797
POL	0.7289	0.9837	0.432	1	0.4139	0.1879	0.1405	0.0642	0.3989
logP	0.1426	0.377	0.0624	0.4139	1	0.0245	-0.0435	-0.101	-0.0839
HOMO	-0.0477	0.1856	-0.2605	0.1879	0.0245	1	0.2127	-0.0635	0.2176
LUMO	0.1194	0.0786	0.0133	0.1405	-0.0435	0.2127	1	-0.0752	0.2457
DM	0.264	0.1178	0.3181	0.0642	-0.101	-0.0635	-0.0752	1	0.2068
lnIC$_{50}$	0.0643	0.3652	-0.0797	0.3989	-0.0839	0.2176	0.2457	0.2068	1

From the correlation matrix it is clear molar refractivity and polarizability have moderately high correlation with ln IC_{50}. Partition coefficient and van der Waals surface area has very low correlation. HOMO, LUMO and Dipole moment has moderate correlation.

A multivariate regression was performed using eight (8) different indices by stepwise addition method [23]. Since HOMO and LUMO plays an important role in transition as well as reaction so we consider these two indexes as our initial step. Using these two quantum chemical parameters Model 1 (Table 4) was constructed and shows a lower F value and correlation coefficient.

Table 4: Regression equations and Fischer F-value using different indices

Model No.	Regression equations	r	r^2	F
Model 1	$\ln Ic_{50} = 9.728269 + (7.6253)HOMO + (27.6314)LUMO$	0.298	0.089	3.57
Model 2	$\ln Ic_{50} = 9.054719 + (8.1413)HOMO + (7.6253)LUMO + (0.1561)DM$	0.379	0.144	7.76
Model 3	$\ln IC_{50} = 9.304326 + (-0.1809)\log P + (8.2142)\text{HOMO} + (29.2211)\text{LUMO} + 0.1523)\text{DM}$	0.383	0.147	10.3
Model 4	$\ln IC_{50} = (-10.881087) + (5.9332)\text{POL} + (-0.7994)\text{logP} + (5.1477)\text{HOMO} + (21.2275)\text{LUMO} + (0.1146)\text{DM}$	0.547	0.299	19.9
Model 5	$\ln IC_{50} = 0.29 + (-17.8827)\text{SASA} + (8.1232)\text{VSA} + (19.6404)\text{Pol} + (-1.4596)\text{logP} + (2.4232)\text{HOMO} + (31.0984)\text{LUMO} + (0.1962)\text{DM}$	0.757	0.573	29.1
Model 6	$\ln IC_{50} = (-0.9232) + (-18.1715)\text{VSA} + (2.3851)\text{MR} + (8.1614)\text{SASA} + (17.4222)\text{POL} + (-1.4521)\text{logP} + (2.1142)\text{HOMO} + (32.8694)\text{LUMO} + (0.1934)\text{DM}$	0.758	0.575	31.2

ln IC_{50}- natural logarithm of Ic50, HOMO- value of HOMO energy, LUMO- value of LUMO energy, DM- dipole moment, SASA-solvent accessible surface area, VSA- van

der Waals surface area. MR- molar refractivity, POL- polarizability, LogP-octanol/water partition coefficient.

In the next step together with HOMO, LUMO we introduce dipole moment (DM). As a result it shows a higher F (7.76) and r (0.379) value than previous one. To modify the results we introduce logP (Model 3) in Model 2. It shows a higher r^2 and F value. polarizability, solvent accessible surface area (SASA), van der Waals surface area (VSA) are added stepwise in Model 4 and Model 5. Model 5 shows a larger r (0.757) and F (29.11) value than Model 4. From this step it is clear that solvent accessible surface area and van der Waals surface area plays an active role in activity. Finally with Model 5 molar refractivity is introduced and constructed Model 6. Model 6 exhibits slightly greater r value (0.758) but modified F (31.29) value. The model 6 having good correlation coefficient value (0.758) explains 57.5% variance in the anthrax lethal toxin inhibitory activity. A satisfactory QSAR model (model 6) was obtained with LOO cross-validation values of 0.56. The higher F value indicate the model is statistically more significant than the other model but model 6 and model 5 both r, r^2, F values are very closes to each other which indicate that little contribution of molar refractivity on regression equation. Therefore steric effect does not improve the activity of hydoxamate inhibitor. Experimental activities and predicted activities of training set represented in Table 5. The predicted biological activities of the compounds in the test set using model 6 are presented in Table 6 with experimental activities and R^2_{pred} for test is 0.267.

Table 5: Values of experimental $lnIC_{50}$ and predicted $lnIC_{50}$ of training set using model 6

Compd No.	$lnIC_{50}$	$lnIC_{50}$ (Model 6)
1	6.8024	7.128667
2	8.0392	7.647253
3	7.6497	8.522042
4	9.8574	9.905629
5	7.0031	6.022826
6	8.7948	8.668462
7	7.9374	7.763879
8	5.6699	6.943415
9	8.0064	5.891324
10	5.9915	6.143184
11	4.8675	5.665155
12	8.5526	6.995867
13	9.3826	9.097739
19	6.697	5.751855
20	4.8675	4.816607
21	4.6052	6.279258
22	4.2485	5.260135
23	5.7038	6.02852
24	4.7875	5.785872
25	4.8675	6.028028

Table 6: Values of quantum chemical indices, experimental and predicted (using Model 6) value of ln IC_{50} of test set

Compd No.	VSA	MR	SASA	POL	logP	HOMO	LUMO	DM	$lnIC_{50}$	$lnIC_{50}$ (Model 6)
26	6.1422	4.3686	6.2372	3.4634	2.105	-0.2146	-0.0449	5.8735	4.1589	5.276187
27	6.0387	4.4252	6.0776	3.5092	2.611	-0.2021	-0.0567	8.7496	3.6376	6.234704
28	6.1003	4.4116	6.2636	3.4624	1.917	-0.1599	-0.0541	9.5845	3.912	7.125803
29	6.1722	4.3954	6.2541	3.4881	1.08	-0.2164	-0.0418	4.8182	3.9889	6.750255
30	5.8979	4.3357	5.9139	3.4241	0.809	-0.1224	-0.0219	3.5729	4.7875	8.711773
31	5.8965	4.3325	5.9143	3.4135	1.947	-0.2207	-0.0366	3.8311	4.2047	6.253476
32	6.1393	4.3325	6.2605	3.4206	1.947	-0.2151	-0.0514	8.1483	4.2047	5.131939
33	6.0846	4.3095	6.2236	3.3995	1.463	-0.2386	-0.0405	1.2967	3.9318	5.118746
34	5.9663	4.3679	6.0579	3.4706	1.939	-0.2074	-0.0535	7.2957	4.1744	7.375374

Hydroxamate analogue (1) exhibit high activity against anthrax lethal toxin. When hydrogen atom of amino group replaced by methyl pyridinyl, ethyl thophenyl, ethyl imidazolyl group of hydroxamate inhibitor (1) of table 1, exhibited high value of inhibition activity, which is evident from the hydroxamate derivatives (2, 3, 4). When methoxy group is replaced by fluorine atom (8), the inhibition activity was reduced. But fluorine atom present at ortho and meta position of phenyl ring (6, 7) displayed high activity. Introduction of methyl group at the para position of phenyl ring (9) would improve the inhibition activity. But methyl group present at the meta position of phenyl ring (10), the activity decreases. Replacing benzene ring with ethyl phenyl group (13) and Chloro benzyl group (14) displayed outstanding activity. When isopropyl group substituted by ethyl, butyl, t-butyl, cyclopropyl, cyclobutyl and similar groups (20-34), are reduced the inhibition activity towards anthrax lethal toxin. On the basis of these

observations we have designed 17 inhibitors and calculated their activity using Regression model 6 exhibits in Table 7. It is found that designed compounds are significant value of inhibition activity (Table 8).

Table 7: Chemical structure of designed compounds

Compd No.	R_1	R_2	R_3
d1	$-CH(CH_3)_2$	-H	4-Nitro-C_6H_5
d2	$-CH(CH_3)_2$	-H	4-$N(CH_3)_2$-C_6H_5
d3	$-CH(CH_3)_2$	4(Pyridnyl)-CH_2-CH_2	4- OCH_3-C_6H_4
d4	$-CH(CH_3)_2$	3-CH_2-Thiophenyl	4- OCH_3-C_6H_4
d5	$-CH(CH_3)_2$	-H	$2CH_3$-C_6H_5
d6	$-CH(CH_3)_2$	-H	4-CCl_3-C_6H_5
d7	$-CH(CH_3)_2$	-H	2-(2F-C_6H_5) Ethyl
d8	$-CH(CH_3)_2$	-H	4-SH-3-CH_3-C_6H_5
d9	$-CH(CH_3)_2$	-H	4-F-3-(CH_2-SH)-C_6H_5
d10	$-CH(CH_3)_2$	-H	4-OCF_3-C_6H_5
d11	2(2-Oxo pyrimidinyl)	-H	4-F-3-CH_3-C_6H_5
d12	$-CH(CH_3)_2$	$-CH_2$-(2-Oxopyridinyl)	4- OCH_3-C_6H_4
d13	$-CH(CH_3)_2$	$-CH_2$-(4NO2-C_6H_5)	4- OCH_3-C_6H_4
d14	$-CH(CH_3)_2$	4- Methoxy- benzyl	4- OCH_3-C_6H_4
d15	$-CH(CH_3)_2$	-H	4(NH_2-CO-NH)C_6H_5
d16	$-CH(CH_3)_2$	-H	4(NH_2-CS-NH)C_6H_5
d17	$-CH(CH_3)_2$	-H	4(NH_2-CO-NH-NH)C_6H_5

Table 8: Designed compounds and their predicted $\ln IC_{50}$ using Model 6.

Compd No.	VSA	MR	SASA	POL	logP	HOMO	LUMO	DM	$\ln IC_{50}$
d1	6.0766	4.2986	6.1874	3.3629	0.863	-0.2698	-0.1244	2.0264	2.474801
d2	6.1779	4.3908	6.2804	3.4637	1.006	-0.1244	-0.0324	11.7828	8.379723
d3	6.403	4.6525	6.4824	3.7243	1.721	-0.1024	-0.0307	7.5891	9.355408
d4	6.3271	4.5987	6.3447	3.6736	2.192	-0.2015	-0.0475	7.9294	7.219331
d5	6.054	4.2671	6.2052	3.3596	1.305	-0.233	-0.0264	7.0286	6.522726
d6	5.8884	4.463	5.9371	3.5683	2.723	-0.1991	-0.0876	6.7121	7.386881
d7	5.9017	4.3285	5.9257	3.4362	1.291	-0.2393	-0.0117	5.7886	8.740487
d8	6.1042	4.3735	6.2703	3.4638	1.51	-0.2388	-0.0504	0.4293	5.835871
d9	5.8844	4.3737	5.9317	3.465	1.287	-0.1256	-0.0397	3.7106	8.637351
d10	6.1344	4.2391	6.2477	3.4006	1.874	-0.201	-0.0389	6.0376	4.69501
d11	6.0601	4.3939	6.1824	3.4247	-0.601	-0.1203	-0.0404	5.4162	9.896373
d12	6.3268	4.6096	6.334	3.6861	0.282	-0.0789	-0.0368	4.9994	10.19898
d13	6.4303	4.6966	6.4724	3.7443	2.563	-0.2288	-0.0785	14.2525	7.458973
d14	6.4424	4.6887	6.5033	3.7598	2.661	-0.1998	-0.0411	8.2498	7.7299
d15	6.1249	4.3797	6.2087	3.4527	0.038	-0.1051	-0.0224	4.954	8.993963
d16	6.1355	4.4751	6.2037	3.5119	-0.059	-0.1956	-0.0528	12.4105	10.41185
d17	6.1726	4.4193	6.2776	3.4792	-0.203	-0.111	-0.0276	5.4492	9.507978

6.4: References

1. Smith H (1954) Observations on Experimental Anthrax: Demonstration of a Specific Lethal Factor produced in vivo by Bacillus anthracis. J Keppie. *Nature*.**173**: 869.

2. Hanna P (1998) Anthrax pathogenesis and host responseCurr. *Top. Microbial. Immunol.*, **225**: 13-35.

3. Liu S, Schubert RL, Bugge TH, Leppla SH (2003) Anthrax toxin: structures, functions and tumour targeting. *Expert OpinBiolTher.*, **3**: 843-853.

4. SH Leppla (2006) Bacillus anthrasis toxins. The Comprehensive sourcebook of bacterial Protein Toxins. EdsAlouf JE, Popoff MR (Acadamic, Burlington, MA) 323-347.

5. Young JA, Collier RJ (2007) Anthrax toxin: Receptor-binding, internalization, pore formation, and translocation. Annu Rev Biochem.,**76:** 243-265

6. Brossier F, M Mock(2001) Toxins of Bacillus anthrasis. Toxicon**39**:1747-1755.

7. Petosa C, Collier RJ, Klimpel KR, Leppla SH, Liddington RC (1997) Crystal structure of Anthrax toxin protective antigen. *Nature*.**385**: 833-838.

8. Bradley KA, MogridgeJ, Mourez M, CollierRJ, YoungJA(2001) Identification of the cellular receptor for anthrax toxin. *Nature*.**414**: 225-229

9. Lacy DB, WigelsworthDJ,ScobieHM, YoungJA, CollierRJ (2004) Crystal structure of the von Willebrand factor A domain of human capillary morphogenesis protein 2: an toxin receptor. *Proc. Natl. Acad. Sci. USA*.**101**: 6367-6372

10. Wigelsworth DJ, KrantzBA, KA ChristensenKA, LacyDB, JurisSJ, CollierRJ(2004) Binding stoichiometry and kineticks of interaction of human anthrax toxin receptor. CMG2, with protective antigen *J. Biol. Chem.*.**279**: 23349-23356

11. Scobie HM, Rainey GJ, Bradley KA, Young, JA. (2003) Human capillary morphogenesis protein 2 function as an anthrax toxin receptor. *ProcNatlAcadsci U.S.A.* **100**: 5170-5174.

12. Leppla SH (1982), Anthrax toxin edema factor: A bacterial adenylatecyclase that increases cyclic AMP concentrations of eukaryotic cells. *ProcNatl Acad. U.S.A.* **79:** 3162-3166.

13. Vitale G,Pellizzari R, Recchi C, Napolitani G, Mock M et al. (1998) Anthrax lethal factor cleaves the N- terminus of MAPKKS and induces tyrosine/threonine phosphorylation of MAPKKs in cultured macrophages. Biochem. biophys. *Res. Commun***248**: 706-711

14. Duesbery NS, Webb CP, Leppla SH, Gordon VM, Klimpel KR, et al. (1998)Proteolytic inactivation of MAP-kinase-kinase by Anthrax lethal factor G.F. *Science.* **280**: 734-737.

15. Pellizzari R, Guidi-Rontani C, Vitale G, Mock M, Montecucco C (1999) Anthrax lethal factor cleaves MKK3 in macrophages and inhibits the LPS/IFNgamma-induced release of NO and TNFalpha.FEBS Lett.,**462:**199–204.

16. VITALE G, BERNARDI L, NAPOLITANI G, MOCK M, MONTECUCCO C (2000)*Biochem. J.*, **352**:739-745.

17. Vitale G, Pellizzari R, Recchi C, Napolitani G, Mock M, et al. (1998) *Biochem. Biophys. Res. Commun.* 248: 706–711.

18. Thomas M, Castignetti D (2009) Examination of anthrax lethal factor inhibition by siderophores, small hydroxamates, and protamine. *J MicrobiolImmunol Infect.*, **42**: 284-289.

19. Chen X, Liu M, GilsonMK (2001) Binding DB: A web-accessible molecular recognition database J. Combi. *Chem. High-Throughput Screen.* **4**: 719-725.

20. Chen X, Lin Y, Gilson MK (2002) The Binding Database: Overview and User's Guide. *Biopolymers NucleicAcid Sci.*, **61**: 127-141.

21. Chen, X., Liu, M., Gilson, MK. (2001) The binding database: Overview and user's guide *Biopolymers/Nucleic Acid Sci.*,**61**: 127–141.

22. Schmidt MW, Baldridge KK, Boatz JA, Elbert ST, Gordon MS, et al. (1993) General atomic and molecular electronic structure system*J Comput Chem.*, *14*: 1347-1363.

23. Padavala AB, Prasanth VV, Jayanthi SA, Vadlamani A, Chitti S (2010) QSAR analysis and validation studies on substituted spiropiperidines as GlyT1 inhibitors*J. Chem. Pharm. Res.*, **2**: 147-162.